ChemComm



COMMUNICATION

View Article Online



Cite this: Chem. Commun., 2024. **60**, 7073

Received 19th April 2024, Accepted 28th April 2024

DOI: 10.1039/d4cc01868k

rsc.li/chemcomm

Regulating iminophosphorane P=N bond reactivity through geometric constraints with cage-shaped triarylphosphines†

Lei Hu,‡§^{ab} Sayandip Chakraborty,§^a Nikolay Tumanov, ¹

Da Johan Wouters,^a Raphaël Robiette ** and Guillaume Berionni **

Structure-reactivity investigations and quantum-chemical parametrization of steric and electronic properties of geometrically constrained iminophosphoranes enabled the design of new frustrated Lewis pairs and revealed unusual properties at the phosphonium center embedded in the cage-shaped triptycene tricyclic scaffold.

Iminophosphoranes, the nitrogen analogues of phosphorus ylides in aza-Wittig reactions, are increasingly used to design pincer type ligands for transition-metals² and main-group elements.³ They have found recent applications in organocatalysis⁴ and in the phosphine-mediated redox catalyzed Staudinger ligation of carboxylic acids and azides (Scheme 1a).⁵ Iminophosphoranes are prepared by the Staudinger reaction, 1a whose reaction intermediates have been extensively investigated (Scheme 1b).

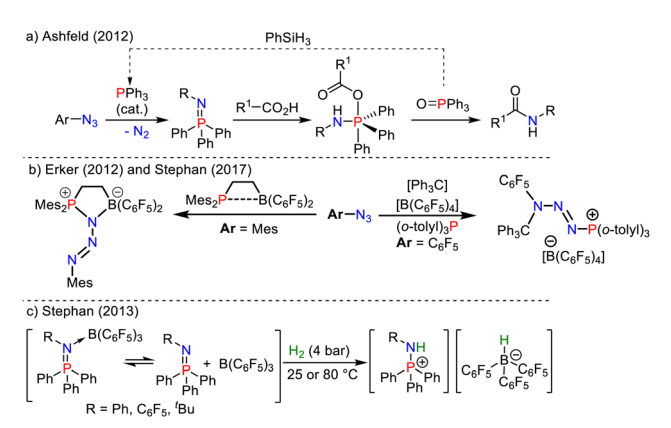
Owing to the high basicity of their nitrogen atom, iminophosphoranes have been extensively used to design superbases (e.g. Schwesinger phosphazenes),7 and have been combined with bulky boron Lewis acids such as B(C₆F₅)₃ to generate frustrated Lewis pairs (FLPs) reacting with small molecules such as CO₂ and H₂ (Scheme 1c).8

Whereas the reactivity of these phospha-aza ylides is usually governed by the electronic and steric properties of the substituents at the P and N atoms, constraining their geometry with a highly strained skeleton or cage-shaped framework is of increasing interest for modulating the reactivity of p-block compounds and reaching new reactivities (Scheme 2).9

Chitnis and coworkers recently designed phosphaza-adamantane with thermal, air, and redox stability by using a geometrically constrained adamantane scaffold (Scheme 2a-A). 10 Radosevich and coworkers modulated the properties of the P=N bond in phosphazenes by designing phosphabicyclic compounds with distorted T-shaped molecular geometries, enabling the tuning of their reactivity via a geometric constraint (Scheme 2a-B). 11 Uchiyama recently employed a phospha-boratriptycene cageshaped scaffold to intercept betaine intermediates in Wittig reactions of phosphorus ylides with aldehydes (Scheme 2a-c). 12

We now report a series of phosphatricyclic nitrogen-ylides derived from 9-phosphatriptycene, 13 in which the geometric constraint is inducing an unusual pyramidalized phosphorus environment at the edge of the triptycene scaffold. 14 The impact of the geometrical constraint on the Lewis and Brønsted basicities, steric hindrance and reactivity of the P=N bond was elucidated by quantitative investigations of their association with carbenium ions, and Brønsted and Lewis acids.

Adducts featuring unprecedented non-covalent fluorine or oxygen non-covalent bonding to C-P σ^* orbitals were obtained



Scheme 1 (a) P^{III}/P^V-redox catalyzed Staudinger ligation reaction.⁵ (b) Interrupted Staudinger reactions.⁶ (c) Applications of iminophosphoranes in FLP chemistry.8

^a Université de Namur, Department of Chemistry, Namur Institute of Structured Matter (NISM), Rue de Bruxelles 61, Namur 5000, Belgium. E-mail: guillaume.berionni@unamur.be

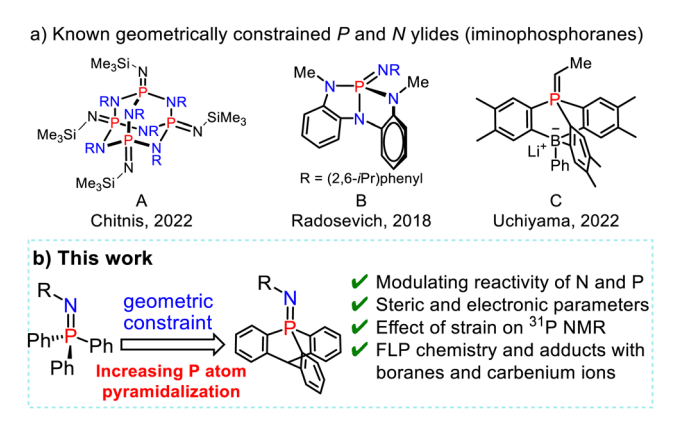
^b Université Catholique de Louvain, Institute of Condensed Matter and Nanosciences, Place Louis Pasteur 1 box L4.01.02, Louvain-la-Neuve 1348, Belgium. E-mail: raphael.robiette@uclouvain.be

[†] Electronic supplementary information (ESI) available. CCDC 2313762-2313774 and 2347266-2347270. For ESI and crystallographic data in CIF or other electronic format see DOI: https://doi.org/10.1039/d4cc01868k

[‡] Current address: Xiamen Key Laboratory of Marine Medicinal Natural Product Resources, Xiamen medical college, Xiamen 361023, P. R. China,

[§] These authors contributed equally to this work.

Communication ChemComm



Scheme 2 (a) Examples of geometrically constrained phosphorus frameworks. (b) This work: exploiting geometric distortion at phosphorus to modulate the P=N bond reactivity and steric hindrance.

and the striking reactivities of the cage-shaped phosphinimines were further exploited to design FLPs with bulky Lewis acids.

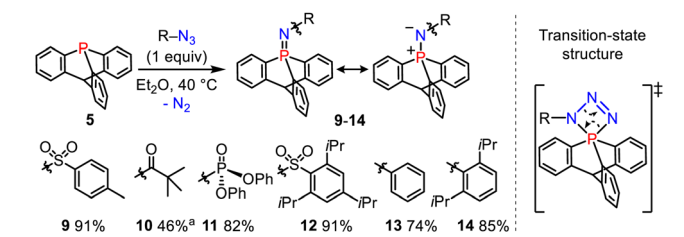
We first compared the magnetic and structural properties of triphenylphosphine 2-4 and triptycene chalcogenides 6-8 (Table 1). Single-crystal X-ray diffraction analysis revealed that TripP=E derivatives 6-8 exhibited a larger pyramidalization angle α than in classical Ar₃P=E derivatives 2-4, corresponding to larger CPC angles of 107.7° versus 97.7°. In ³¹P NMR spectroscopy, a large shielding is observed between the 9-phosphatriptycene 5 (-64.4 ppm) and Ph₃P 1 (-4.7 ppm), while a smaller shielding was observed between Trip-P=E and Ph₃P=E derivatives (Table 1). Consistent with the literature, ^{14e} the ¹J ³¹P-⁷⁷Se of 822 Hz in 8 is nearly 100 Hz larger than for PPh₃=Se 4 (729 Hz) indicating that the overall donating ability of phosphatriptycene 5 is less than Ph₃P. 13a Compound 6 was found to stabilize a molecule of H₂O₂ (Fig. S1 in the ESI†).

We then performed the Staudinger reactions of 9-phosphatriptycene 5 with several azides R-N3 to synthesize the cageshaped iminophosphoranes 9-14 (Scheme 3). According to the classical mechanism, 15 these reactions are likely proceeding via

Table 1 Phosphorus-element bond lengths (in Å), pyramidalisation at the P atom (angle α in $^{\circ}$) and 31 P NMR chemical shifts (δ in ppm) in triphenylphosphine 1-4 and phosphatriptycene 5-8 derivatives

Chalcogenide de	O	S	Se		
Triphenylphosph	ine P–E α^a δ^{31} P ppm	1 — 26.1 ^{14a} -4.7	2 1.482 (3) 22.4 ^{14b} 29.2 ^{14c}	3 1.955 (7) 22.9 ^{14d} 43.3 ^{14e}	4 2.114 (8) 22.6 ^{14g} 35.3 ^{14f}
Phosphatriptycer	5	6	7	8	
Ë	Р-Е	_	1.482(1)	1.941(1)	2.091(1)
	$\stackrel{\alpha}{\delta}$ ³¹ P ppm	29.8 -64.4 ^{14h}	28.7 7.32	29.2 12.72	29.1 4.52

^a Pyramidalization angle α defined as the angle between the C–P bonds and the plane formed by the ipso-carbon atoms of the triptycene aryl rings, see ESI.



Synthesis of the 9-phosphatriptycene-imines **9–14**. ^a Pre-Scheme 3 pared with different synthetic procedures, see the ESI† for more details.

an unusual inorganic spiro-cyclic transition-state with a fourmembered PNNN ring connected to a phosphabicyclo[2.2.2]octane tricyclic core.

The 31 P NMR chemical shifts of 9-14 (-5 to -33 ppm) were again more shielded than in the corresponding Ph₃P=NR derivatives reported in the literature (0 to 15 ppm).¹⁴ The formal P=N double bond has predominantly an ylidic nature (see right-hand side resonance structure, Scheme 3) as confirmed by NBO calculations showing that the short PN bond lengths are resulting from negative hyperconjugation between the N lone pairs and σ_{P-C}^* antibonding orbitals (2nd order perturbation stabilization energy E2 = 9.8, 33.2 and 33.3 kcal mol^{-1} for 13). 16

X-ray crystallographic analysis of compounds 9–14 (see ESI†) revealed a high pyramidalization angle at P, e.g. $\alpha = 29.0^{\circ}$ in 13 and only 23.3° for its Ph₃P=NPh analogue (Fig. 1a and b).

Compound 10 has a P···O distance (2.717(3) Å) well under the van der Waals radii of both atoms (represented by the red and vellow wireframe spheres around O and P, respectively, Fig. 1c), implying a preponderant resonance structure with marked electrostatic interaction between the positively charged P atom and negatively charged O atom (Fig. 1d).

This interaction is also confirmed by the NBO analysis of 10, which reveals an electronic interaction between one lone pair of the oxygen atom and one σ_{P-C}^* bond (E2 = 2.2 kcal mol⁻¹). Due to the cage-shaped structure of phosphatriptycene, this P-distance is significantly shorter than in any previous reported

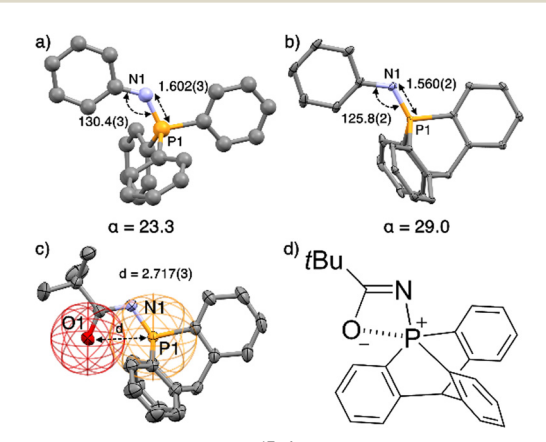


Fig. 1 (a) Structure of Ph₃P=NPh^{17e,f} and (b) of its analogue 13 with key geometrical features. (c) Ellipsoid representation of single crystal X-ray structures of 10; H atoms and solvent are omitted for clarity. (d) Preponderant mesomeric structure of 10. Distances in Å, angles in °, pyramidalization anale α in °.

ChemComm Communication

$$\bigcap_{\mathsf{NTf}_2} \mathsf{Ph} \longrightarrow \bigcap_{\mathsf{NTf}_2} \mathsf{Ph} \longrightarrow \bigcap_{\mathsf{CD}_2\mathsf{Cl}_2,\,\mathsf{RT}} \mathsf{Ph$$

Scheme 4 Reaction of 13 with a Brønsted and a boron Lewis acid

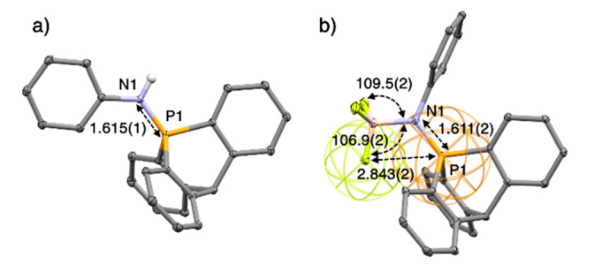


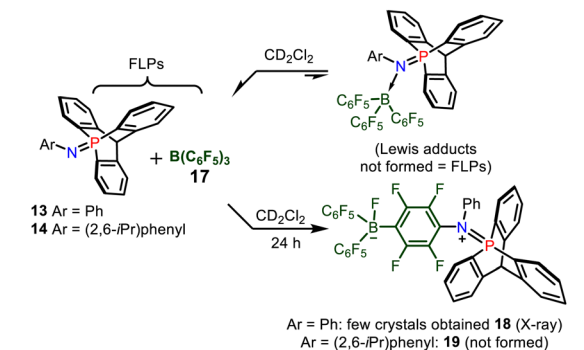
Fig. 2 Ellipsoid representation (50% probability level) of single-crystal X-ray structures of one of the two molecules in the asymmetric unit of 15 (a), and 16 (b). H atoms, anion and solvent are omitted for clarity

phosphorus imidates (previous shortest = 2.848(2) Å for the corresponding Ph₃P=NCOtBu analogue of 10).¹⁷

The iminophosphorane 13 was used for subsequent reactivity studies and was reacted with triflimidic acid HNTf2 and BF3. OEt₂ giving respectively 15 and 16 in good yields (Scheme 4). Protonation and BF₃ complexation induced a deshielding of the ³¹P NMR signals of **15** (10.7 ppm) and **16** (10.4 ppm) compared to that of 13 (-20.4 ppm). Crystallographic analysis showed that H⁺ and BF₃ complexation of 13 resulted in a significant P-N lengthening, with a PN distance of 1.560(2) Å in 13, 1.615(1) Å in 15 and 1.611(2) Å in 16 (Fig. 2). This can be accounted for by the loss of one lone pair on the nitrogen that decreases the hyperconjugation with the σ_{P-C}^* orbitals (E2 = 13.3 and 13.5 kcal mol⁻¹ for 15) as compared to what was observed in 13 (vide supra).

The structure of 16 in the solid state revealed that one F atom in BF₃ is anti ($\theta_{C-P-F} = 173.65(8)^{\circ}$) to one of the P-C_{arom} bonds (Fig. 2b). The valence angle θ_{N-B-F} for F_1 is 106.9(2)°, whereas it is 109.5(2)° and 109.8(2)° for the other two fluorine atoms. This suggests an interaction between the lone pair of one fluorine with the σ^* orbital of one $C_{arom}\text{--P}$ bond. This $P\!\cdot\cdot\cdot F$ distance of 2.8433(14) Å is longer than in the phosphonium based anion receptors of Gabbaï (2.666(2) Å) in which the phosphonium bears a positive charge. 18 Nevertheless, it is still very short with a F...P distance in 16, well below the sum of the van der Waals radii of both atoms (3.35 Å), represented by wireframe coloured spheres around F and P (Fig. 2b).

Then, the association of 13-14 with tris(pentafluorophenyl)borane 17 was investigated by multinuclear NMR spectroscopy (Scheme 5). When mixing these reagents in CDCl₃, a negligible deshielding of the signal of 13 (\approx 3 ppm) was observed by ³¹P NMR spectroscopy, and only a broadening of the peaks was observed in ¹H NMR, while the ¹¹B NMR signal of **17** remained at -60.0 ppm. This indicated a very weak interaction between 13 and B(C₆F₅)₃ typical of an encounter complex or a frustrated



Scheme 5 FLPs between 13 and 17 and deactivation pathway resulting in the formation of the phospha-iminium fluoroborate 18

Lewis pair, and the formation of a Lewis adduct was thus excluded. After keeping the FLP solution for one day, crystals of compound 18 were obtained (see ESI,† Fig. S2) among other decomposition products. Thus, the deactivation of FLP occurs partly via S_NAr reaction of the nitrogen atom of the 9phospatriptycene imine 13 at the para position of a C₆F₅ ring of $B(C_6F_5)_3$ (Scheme 5), similarly as with phosphorus ylides. 8c In the case of 14, since it is of larger steric hindrance around it's nitrogen atom, such type of S_NAr reaction to yield 19 was not possible.

The steric hindrance at the nitrogen atom was comparable for TripP=NPh (13) and Ph₃P=NPh according to their similar buried volume %V_{bur} and He₈_steric parameters (see ESI,† Table S3).¹⁹ Analogously, the %V_{bur} of phosphatriptycene 5 (31.3%) is comparable to that of Ph₃P **1** (29.6%).²⁰

Computations show that the proton (PA) and methyl cation affinities (MCA) of iminophosphoranes 9-14 are influenced by geometric constraints at the phosphorus atom. This constraint decreases the basicity at N by up to 8 kcal mol⁻¹ when comparing 13 to is analogue Ph₃P=NPh (Table 2). It simultaneously enhances the Lewis acidity at the phosphorus atom by 4 kcal mol⁻¹, as evidenced by fluoride ion affinity (FIA) values at the electron deficient formal phosphonium P centre. Analysis of the fluoride complexation through the activation strain model (see ESI,† Table S4) indicates that this enhanced Lewis acidity is mainly due to a lower distortion energy in the case of 13. The energy necessary for the geometrically constrained phosphatriptycene imine structure to adopt the trigonal

Table 2 Computed proton affinities (PAs) and methyl cation affinities (MCAs) of 9-14 with respect to the N atom in benzene as a solvent in kcal mol⁻¹, and fluoride ion affinities (FIA) in kcal mol⁻¹ with respect to the P atom

	Cmpd B	9	10	11	12	13	14	Ph ₃ P=NPh
PA	263	247	255	246	245	262	264	270
MCA	110	93	95	92	94	108	113	113
FIA^a	60^b	47	37	45	51	36	3.0	32

a Computed FIA at the pseudo phosphonium center using the isodesmic approach with COF₂ anchor points; see ESI, Table S2 for the FSiMe₃ anchor point and for FIAs for 6-8. b In agreement with the reported FIA value for compound B (Radosevich T-shaped iminophosphoranes shown in Scheme 2b) of 57 kcal mol⁻¹ in ref. 11.

Communication ChemComm

Scheme 6 FLP type reaction of iminophosphorane 13 with the tritylium tetrafluoroborate to yield compound 21.

bipyramidal geometry is indeed lower (by 4.6 kcal mol⁻¹) than the one required for Ph₃P=NPh.

Finally, we found that combining 13 with a titylium ion results in a nitrogen/carbon FLP, and the phospha-iminium 20 was not formed (Scheme 6), but instead SEAr reactions occurred at the para position of N-Ph of 13 to yield compound 21, evidenced by X-ray diffraction (Fig. S2b, ESI†).

Thus, in conclusion, the geometric constraints brought by the cage-shaped tricyclic phosphatriptycene scaffold decrease the Brønsted basicity at the nitrogen but enhance the Lewis acidity at the phosphorus, leading to a partial Umpolung type reactivity at the P=N bond. Unusually short non-covalent F···P and O···P intramolecular electrostatic contacts also result from the geometrical constraints. The new cage-shaped phosphatriptycene nitrogen-ylides might have interesting reactivity in terms of frustrated Lewis pairs catalysis²¹ which is subject to further exploration in our labs. The transition metal-free directed electrophilic borylation²² of the triptycene core based on the N-centred directing group approach is also under investigation.

We acknowledge the University of Namur (CERUNA PhD fellowship for S. C.) and the Fond de la Recherche Scientifique FNRS (F.R.S-FNRS) for financial support (Grants T.0012.21 (G. B.) and GEQ UG02222F (J. W.)). Computational resources have been provided by the supercomputing facilities of the Université catholique de Louvain (CISM/UCLouvain) and the Consortium des Équipements de Calcul Intensif en Fédération Wallonie Bruxelles (CÉCI) funded by the F.R.S.-FNRS under convention 2.5020.11 and by the Walloon Region. We thank the PC2 (UNamur) technological platforms for access to all characterization instruments. LH expresses gratitude for the PhD grant support from the China Scholarship Council (CSC, no. 201606670003) and acknowledges the FNRS Mobility Grant for research exchange at the University of Basel. Special appreciation goes to Prof. Olivier Baudoin for hosting and to Dr A. Clemenceau for experimental assistance during this period. RR is a Maître de Recherche of the F.R.S.-FNRS.

Conflicts of interest

There are no conflicts of interest to declare.

Notes and references

- 1 (a) H. Staudinger and J. Meyer, Helv. Chim. Acta, 1919, 2, 635-646; (b) S. P. Marsden, et al., Org. Lett., 2008, 10, 2589–2591; (c) L. Wang, et al., Synthesis, 2015, 3522-3528; (d) H. A. Van Kalkeren, et al., Adv. Synth. Catal., 2012, 354, 1417-1421; (e) H. A. Van Kalkeren, et al., Eur. J. Org. Chem., 2013, 7059-7066; (f) H. Bel Abed, et al., Org. Biomol. Chem., 2014, 12, 7159-7166.
- 2 (a) L. Beaufort, et al., J. Mol. Catal. A: Chem., 2008, 283, 77-82; (b) O. Alhomaidan, et al., Organometallics, 2008, 27, 6343-6352; (c) E. Martinez-Arripe, et al., Organometallics, 2012, 31, 4854-4861; (d) J. García-Álvarez, et al., J. Organomet. Chem., 2014, 751, 792–808.
- 3 (a) T. Cantat, et al., Dalton Trans., 2008, 1957-1972; (b) M. Fustier-Boutignon, et al., Chem. Rev., 2019, 119, 8555-8700; (c) K. Dehnicke and F. Weller, Coord. Chem. Rev., 1997, 158, 103; (d) D. W. Stephan, Adv. Organomet. Chem., 2006, 54, 267.
- 4 D. Rozsar, et al., Angew. Chem., Int. Ed, 2023, 62, e202303391.
- 5 A. D. Kosal, et al., Angew. Chem., Int. Ed., 2012, 21, 12036-12040.
- 6 (a) A. Stute, et al., Chem. Commun., 2012, 48, 11739-11741; (b) J. Zhou, et al., Dalton Trans., 2017, 46, 9334-9338.
- 7 (a) M. Formica, et al., Acc. Chem. Res., 2020, 53, 2235-2247; (b) R. Schwesinger, et al., Angew. Chem., Int. Ed. Engl., 1993, 32, 1361.
- 8 (a) C. F. Jiang and D. W. Stephan, *Dalton Trans.*, 2013, 42, 630–637; (b) J. Y. Zhang, et al., Chin. Chem. Lett., 2018, 29, 1226-1232; (c) S. Döring, et al., Organometallics, 1998, 17, 2183-2187.
- 9 (a) T. S. Barnard and M. R. Mason, Organometallics, 2001, 20, 206-214; (b) S. Tretiakov, et al., Angew. Chem., Int. Ed., 2021, 60, 9618-9626; (c) For a recent review on p-block compounds see: T. J. Hannah and S. S. Chitnis, Chem. Soc. Rev., 2024, 53, 764-792.
- 10 J. Bedard, et al., Angew. Chem., Int. Ed., 2022, 61, e202204851.
- 11 Y.-C. Lin, et al., Chem. Sci., 2018, 9, 4338-4347.
- 12 (a) Y. Uchiyama, et al., J. Org. Chem., 2022, 87, 15899-15913; For further applications of phosphatriptycenes in catalysis and coordination chemistry, see: (b) Y. Cao, et al., Organometallics, 2019,
- 13 (a) L. Hu, et al., J. Org. Chem., 2019, 84, 11268-11274; (b) H. Gildenast, et al., Dalton Trans., 2022, 51, 7828-7837; (c) D. Rottschäfer, et al., Inorg. Chem., 2023, 62, 18228; (d) For the original synthesis of 9-phosphatriptycene, see: C. Jongsma, et al., Tetrahedron, 1974, 30, 3465-3469.
- 14 (a) H. Kooijman, et al., Acta Cryst. C, 1695, 1998, 54; (b) L. R. Falvello, et al., CSD Commun., 2002, CCDC 186887; (c) J. Yang, et al., Chem. Commun., 2016, 52, 12233; (d) C. Foces-Foces and A. L. Llamas-Saiz, Acta Cryst. C, 1998, 54, 9800013; (e) P. W. Codding and K. A. Kerr, Acta Crystallogr., Sect. B: Struct. Crystallogr. Cryst. Chem., 1978, **34**, 3785; (f) R. Kumar, et al., Eur. J. Inorg. Chem., 2018, 1028; (g) A. L. Rheingold, CSD Commun., 2011, CCDC 856709; (h) H. Hu, et al., Dalton Trans., 2021, 50, 4772-4777.
- 15 F. L. Lin, et al., J. Am. Chem. Soc., 2005, 127, 2686-2695.
- 16 A similar analysis was made by Dehnicke, See: H. Folkerts, et al., Angew. Chem., Int. Ed. Engl., 1995, 34, 1362.
- 17 (a) W. Han, et al., Org. Lett., 2022, 24, 6247-6251; (b) C. Larré, et al., Eur. J. Inorg. Chem., 1999, 601-611; (c) J. Yang, et al., Chem. Commun., 2016, 52, 12233; (d) Y. Matano, et al., J. Am. Chem. Soc., 2001, 123, 10954-10965; (e) E. Böhm, et al., Zeit. Naturforsch. B, 2014, 43, 138; (f) I. Bar and J. Bernstein, Acta Crystallogr., Sect. B: Struct. Crystallogr. Cryst. Chem., 1980, 36, 1962-1964.
- 18 T. W. Hudnall and F. P. Gabbaï, J. Am. Chem. Soc., 2008, 130, 10890-10891.
- 19 (a) N. Fey, et al., Organometallics, 2008, 27, 1372-1383; (b) J. Jover, et al., Organometallics, 2012, 31, 5302-5306; (c) D. J. Durand and N. Fey, Chem. Rev., 2019, 119, 6561-6594.
- 20 H. Clavier and S. P. Nolan, Chem. Commun, 2010, 46, 841-861.
- 21 M. G. Guerzoni, et al., Chem. Catal., 2022, 2, 2865-2875.
- 22 (a) S. Rej and N. Chatani, J. Am. Chem. Soc., 2021, 143, 2920-2929; (b) S. A. Iqbal, et al., Chem. Soc. Rev., 2020, 49, 4564-4591.